American Mineralogist, Volume 79, pages 1–8, 1994

Pressure-induced phase transition in cristobalite: An X-ray powder diffraction study to 4.4 GPa

David C. Palmer,* Larry W. Finger

Geophysical Laboratory and Center for High Pressure Research, Carnegie Institution of Washington, 5251 Broad Branch Road NW, Washington, DC 20015-1305, U.S.A.

Abstract

The structural behavior of cristobalite, SiO_2, has been studied under hydrostatic conditions in a diamond-anvil cell to 4.4 GPa, using high-resolution synchrotron X-ray powder diffraction. On increasing pressure, we observed a phase transition at $P_c \sim 1.5$ GPa, characterized by the onset of twinning and the splitting of powder diffraction lines. This transition is reversible and first-order in character. The high-pressure phase, referred to here as cristobalite II, can be indexed according to a monoclinic unit cell with $a = 9.124(5)$, $b = 4.625(3)$, $c = 8.394(5)$ Å, $\beta = 124.91(5)°$, and $V = 290.5(2)$ Å^3 at $P = 3.1$ GPa. The transition from tetragonal α cristobalite to monoclinic cristobalite II involves a doubling of the unit-cell size and must therefore be induced by a zone-boundary instability. The resulting components of the spontaneous strain tensor are analyzed in terms of the change in point group symmetry from 422 to 2 and of coupling with the macroscopic order parameter. There is a significant non-symmetry-breaking (volume) strain. The actual symmetry-breaking process is a shear parallel to $[\bar{1}01]$ in the tetragonal (101) planes, corresponding to slip on the {111} tetrahedral sheets of the high-T cubic β-cristobalite phase.

Introduction

The phase transition behavior of framework silicate minerals has been the subject of major interest in recent years. The concomitant development of mean-field theories of phase transition behavior, microscopic computer modeling, and new experimental techniques probing a range of length scales and dynamical phenomena has facilitated a profound reevaluation of structural behavior in complex silicates. Many common rock-forming aluminosilicates exhibit diverse structural behavior with changing temperature (and presumably also with changing pressure), such as cation order-disorder processes (e.g., Al-Si), and elastic instabilities that lead to displacive phase transitions. The coupling between individual order parameters, often by means of a common lattice strain, can make the overall behavior very complex.

One way in which the resulting behavior can be rationalized is by comparison with well-characterized model systems, which exemplify particular aspects of structural behavior. Many phase transitions involve distortions of the aluminosilicate framework. Attention has therefore been focused on similar distortions observed in the tetrahedral framework structures of pure SiO_2 polymorphs in the absence of cation ordering effects, cation mobility, etc. The expectation is that these phases are most likely to epitomize the intrinsic behavior of SiO_2 linkages.

Cristobalite is a high-temperature polymorph of SiO_2, generally associated with the late stages of crystallization in volcanic rocks. In common with tridymite (with which it is often associated in nature), cristobalite is metastable under standard conditions, the expected reconstructive transformation to the equilibrium polymorph, quartz, being kinetically hindered. The crystal structure of cristobalite comprises a three-dimensional network of corner-sharing SiO_4 tetrahedra. Each O atom is a bridging O atom, and so the structure is a fully polymerized tetrahedral framework. The SiO_4 tetrahedra are arrayed in six-membered rings, within close-packed layers, stacked parallel to [111], with three-layer, ABCABC . . . repeat. (This idealized cubic structure is analogous to that of diamond, with the C-C bond replaced by Si-O-Si.)

At high temperatures cristobalite shows macroscopic cubic symmetry, and an aristotype structure of space group $Fd3m$ is inferred, although the microscopic nature of this phase is the subject of some debate (Wright and Leadbetter, 1975; Hatch and Ghose, 1991; Schmahl et al., 1992; Swainson, 1992). On decreasing temperature there is a first-order displacive phase transition to a tetragonal form with space group $P4_12_12$. This phase transition involves a large spontaneous strain (~4%), which can cause some single crystals to fracture (Schmahl et al., 1992). Recent theoretical analysis (Swainson, 1992; Dove et al., 1992; Giddy et al., 1993) suggests that this phase transition is due to the condensation of a low-lying rigid-unit mode.

Early evidence for an additional structural phase transition, occurring at high pressures, came from unpub-

* Present addresses: Emmanuel College, Cambridge, CB2 3AP, England, and Department of Earth Sciences, University of Cambridge, Downing Street, Cambridge CB2 3EQ, England.

0003–004X/94/0102–0001$02.00

lished Raman spectroscopy experiments (Russell Hemley, personal communication), which showed the splitting of certain modes above $P \sim 2.0$ GPa. These findings were confirmed by later, more detailed Raman spectroscopy experiments (Palmer et al., 1991). The first direct evidence for a structural phase transition was reported by Yeganeh-Haeri et al. (1990), who used energy-dispersive X-ray diffraction on a powdered sample in a large-volume press. They observed the splitting of certain diffraction lines at $P_c \sim 1.0$ GPa, which suggested a phase transition to a new phase with lower symmetry. The authors noted that the phase transition appeared to be second-order and nonquenchable but were unable to index the high-pressure phase. This low-pressure phase transition was not detected in another diffraction study on cristobalite (Tsuchida and Yagi, 1990), which nevertheless managed to uncover two other phase transitions at the higher pressures of 10 and 30–40 GPa. Again, the nature of the high-pressure phases remained a mystery.

Our own study is part of a long-term investigation concerned with the pressure dependence of structural behavior in tectosilicates. We focus on the low-pressure phase transition in cristobalite to illuminate possible framework distortions that may occur in other, commonly occurring tectosilicates at moderate pressures.

Experimental

The sample used for this work is cristobalite from the Ellora Caves, near Hyderabad, India (Harvard Mineralogical Museum, no. 97849), and is described by Van Valkenburg and Buie (1945) and Wolfe (1945). The crystals formed in a hydrothermal vein, nucleating on fibers of the zeolite mordenite. Most of the cristobalite crystals are gem-quality octahedra, about 0.5 mm in diameter, some with interpenetrant growth twins. In addition, the crystals are very heavily twinned on a microscopic scale, presumably as a result of the cubic-tetragonal phase transition at $T_c \sim 220$ °C. The same sample has been used in a number of other studies (Dollase, 1965; Peacor, 1973; Yeganeh-Haeri et al., 1992; Downs and Palmer, 1994).

For these experiments, a single cristobalite octahedron was crushed to a fine powder, and transferred to Merrill-Bassett-type diamond-anvil cell. We used an Inconel alloy gasket, between opposing diamond crystals with 600-μm culets. A 4:1 methanol to ethanol mixture was the hydrostatic pressure medium. Pressure calibration was achieved by measuring the laser-induced fluorescence of tiny ruby chips scattered throughout the sample chamber and correlating it with the ruby pressure scale of Mao et al. (1978). Because of the relatively low pressures in this study, we put great emphasis on trying to ensure a consistent and relatively accurate pressure calibration. Ruby fluorescence spectra were fitted using least-squares profile refinement, with Lorentzian functions for the R1 and R2 peaks. Absolute calibration was achieved with reference to a ruby 1-atm standard, measured in an identical manner to the sample at pressure. In these experiments, pressure gradients were all less than the experimental precision of ± 0.5 kbar.

Synchrotron X-ray diffraction experiments were carried out at beam line X7A of the National Synchrotron Light Source, Brookhaven National Laboratory, New York. Monochromatic X-radiation of wavelength $\lambda \sim 0.7$ Å was selected with a curved, asymmetrically cut Si(111) or Ge(111) monochromator crystal. The diamond-anvil cell was mounted with its axis parallel to the incident X-rays, and this orientation was maintained throughout the experiment. The scattered X-rays were measured by scanning a detector through 2θ. Two types of detectors were used during this work: a conventional, single-channel Kevex detector and a linear position-sensitive detector. The position-sensitive detector allowed simultaneous data collection within a diffraction window of 2° 2θ, with the detector moved in 2° steps between successive scans. This allowed for relatively fast data collection, at high resolution: $\Delta d/d \approx 0.001$, an order of magnitude better than the best resolution possible from energy-dispersive detectors. Further details about this design may be found in Jephcoat et al. (1992).

Wavelength and $2\theta_0$ calibrations were determined by measuring a CeO_2 reference specimen mounted in the same position as the diamond-anvil cell. The positions of diffraction peaks were determined by least-squares profile refinement, employing a pseudo-Voigt function and an asymmetry correction.

Lattice parameters

X-ray diffraction patterns were collected at five pressures in the diamond-anvil cell, with an additional pattern measured at 1 atm using a laboratory-based Scintag powder diffractometer. At $P \sim 0.7$ GPa the cristobalite remained tetragonal, but, on increasing the pressure to $P = 1.5$ GPa, a dramatic difference was observed in the diffraction patterns. Formerly single tetragonal reflections had split into a cluster of weaker peaks, as illustrated in Figure 1. With a further increase in pressure, the splittings became better resolved, and the diffraction peaks moved to higher angles.

The distinct and sudden splitting of diffraction lines denotes a structural phase transition, as reported by Yeganeh-Haeri et al. (1990) and Palmer et al. (1991). More specifically, the similarity between clusters of peaks in the high-P phase and individual peaks in the low-P phase suggests a definite crystallographic relationship (e.g., subgroup-supergroup) between the two phases. In our own single-crystal study of the tetragonal phase (Downs and Palmer, 1994), we had noticed a transition at $P \sim 1.2$ GPa; slow, ω and $\theta/2\theta$ scans across selected diffraction peaks revealed splittings characteristic of lamellar twinning.

In order to distinguish the various phases of cristobalite at high pressures, we recommend an alternative to the traditional α, β nomenclature. We opt for a numbered system, reflecting the number of symmetry reductions that

the high-temperature aristotype structure might undergo. Other workers, e.g., Tolédano and Tolédano (1987), have already advocated a numbered system, based as it is on a symmetry classification. The phase with highest possible symmetry, i.e., the aristotype, is denoted phase 0, then its subgroups are numbered in succession, with decreasing symmetry. The high-temperature, cubic aristotype structure ($Fd3m$) therefore becomes cristobalite 0, the tetragonal α phase ($P4_12_12$) is cristobalite I, and this new, high-pressure phase is henceforth referred to as cristobalite II.

Indexing the high-pressure unit cell

Although we were able to resolve the separation of tetragonal peaks into a number of components, it was not immediately obvious how the diffraction peaks of the high-P phase could be indexed. The suddenness of the phase transition and the identical profiles displayed by all diffraction peaks at and above this pressure indicated that we were dealing with one specific phase, and not a mixture of two or more phases. [This was confirmed in Raman spectroscopy experiments (Palmer et al., in preparation), which show an abrupt discontinuity in the frequencies of certain modes on moving from one phase to the other. These measurements also indicate that for samples repeatedly cycled through the phase transition, it is possible to observe the coexistence of both low-P and high-P phases within the well-defined hysteresis interval (P_c' = 0.2; P_c = 1.2 GPa), characteristic of a first-order displacive transition.]

Using the TREOR90 computer program (Werner et al., 1985) we were able to index the high-P powder diffraction data automatically on the basis of a monoclinic unit cell. Since the phase transition is a reversible one, apparently displacive, we would expect a simple relationship between the unit cells of low- and high-P phases. In order to compare these unit cells directly, the tetragonal cell must be extrapolated to the corresponding pressure within the stability field of the monoclinic phase. The unit-cell data of Downs and Palmer (1994) for the same (tetragonal) cristobalite sample are used for comparison. A least-squares fit of the third-order Birch-Murnaghan equation of state, with V_0 = 171.1 Å^3, gives values of 11(1) GPa for the isothermal bulk modulus, K_{0T}, and 12(4) for the pressure derivative, K'. By replacing the term V_0/V by the axial ratio a_0/a or c_0/c, we can extrapolate the cell parameters a and c to high pressures. The resulting moduli are K_{0T} = 39(5), K' = 40(20), and K_{0T} = 30 ± 10, K_{0T} = 26(3) GPa for the a and c axes, respectively.

At P = 3.1 GPa, the high-P monoclinic cell is approximately double the volume of the extrapolated tetragonal cell (Table 1). Furthermore, the b cell length is close (within 3%) to the extrapolated a (or b) parameter for the tetragonal cell. In order to facilitate the comparison of the two structures, it is useful to describe the high-pressure cell in terms of a pseudotetragonal cell, with its axes approximately parallel to the axes of the low-P tetragonal

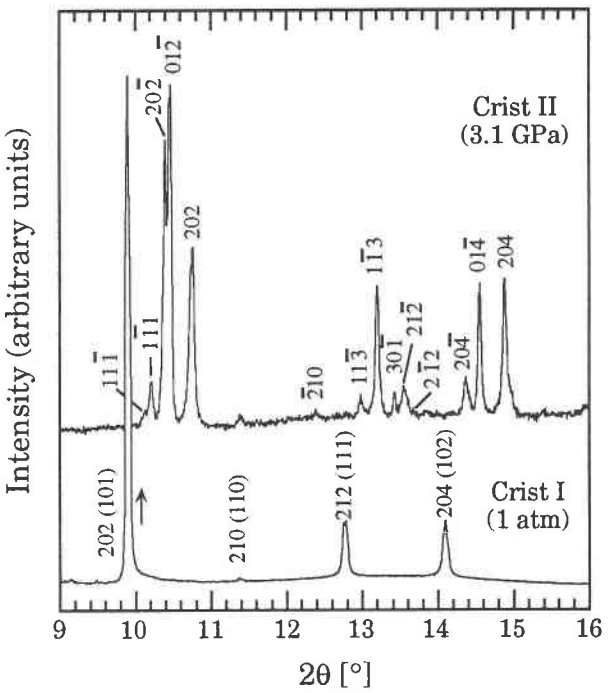

Fig. 1 X-ray diffraction patterns for cristobalite at 1 atm and 3.1 GPa (X-ray wavelength = 0.700 Å). Diffraction peaks are indexed according to the monoclinic B cell of cristobalite II, with the corresponding indices for the tetragonal P unit cell (cristobalite I) given in parentheses.

unit cell. This nonconventional cell is double the volume of the standard cell and is B-face centered. The orientation relation may therefore be expressed as

$$\begin{pmatrix}\mathbf{a}\\ \mathbf{b}\\ \mathbf{c}\end{pmatrix}_{BII} = \begin{pmatrix}1\ 0\ 1\\ 0\ 1\ 0\\ -1\ 0\ 1\end{pmatrix}\cdot\begin{pmatrix}\mathbf{a}\\ \mathbf{b}\\ \mathbf{c}\end{pmatrix}_{PII}. \qquad (1)$$

In the absence of single-crystal diffraction data for the cristobalite II phase, we cannot be absolutely certain of the relative orientations of the cristobalite I and II lattices. However, it is possible to infer the orientation relation by observing how the tetragonal powder diffraction lines split into their monoclinic counterparts (Fig. 1) and noting relationships between the unit-cell parameters. Our proposed relationship between the extrapolated tetragonal unit cell and the monoclinic P (conventional) and B (nonconventional) unit cells is illustrated in Figure 2. The monoclinic B cell is interpreted as a supercell comprising four unit cells of the low-pressure tetragonal cell. The orientational relationship between cristobalite I (tetragonal P) and cristobalite II (monoclinic B) can then be approximated by

$$\begin{pmatrix}\mathbf{a}\\ \mathbf{b}\\ \mathbf{c}\end{pmatrix}_{BII} = \begin{pmatrix}2\ 0\ 0\\ 0\ 1\ 0\\ 0\ 0\ 2\end{pmatrix}\cdot\begin{pmatrix}\mathbf{a}\\ \mathbf{b}\\ \mathbf{c}\end{pmatrix}_{PI}. \qquad (2)$$

TABLE 1. Lattice parameters for cristobalite I and cristobalite II

P (GPa)	a (Å)	b (Å)	c (Å)	β (°)	V (Å^3)
0.0001	½ × 9.950(2)	4.975(1)	½ × 13.848(8)	90	¼ × 658.5(3)
1.61(1)	9.401(9)	4.746(3)	13.890(9)	91.63(4)	618.6(5)
2.04(3)	9.312(9)	4.706(3)	13.83(1)	91.80(5)	605.8(5)
2.81(7)	9.146(96)	4.639(4)	13.792(12)	92.08(5)	584.7(5)
3.05(6)	9.123(5)	4.625(3)	13.775(8)	92.02(4)	580.9(4)
4.37(4)	8.951(2)	4.561(1)	13.743(3)	92.43(1)	560.5(1)

Note: lattice parameters for the tetragonal cell extrapolated to P = 3.05 GPa are a = ½ × 9.554, b = 4.777, c = ½ × 13.046 Å, V = ¼ × 597.6 Å^3. A monoclinic B cell is used for cristobalite II.

The inferred space group of the monoclinic phase is $P2_1$, which is a subgroup of $P4_12_12$; for this case the unit-cell volume doubles at the phase transition, with the driving order parameter relating to an R-point zone-boundary instability (Stokes and Hatch, 1988). The crystal structure has been solved from a combination of DLS and Rietveld techniques and will be presented elsewhere (Palmer and Finger, in preparation). The new structure has a displacive relationship with the low-P form, consistent with the relations presented here.

Pressure-dependence of the lattice parameters

Using the orientation relation between the tetragonal and monoclinic structures, we may directly compare the lattice parameters for α cristobalite (single-crystal data from the same crystals. Downs and Palmer, 1994) and cristobalite II (this study). Figure 3 reveals the abrupt nature of the structural phase transition at $P \sim 1.6$ GPa. The unit cell collapses parallel to **a** and **b**, and the β angle increases dramatically from 90 to 91.6° at the phase transition. Rather intriguingly, the c axis, which is the most compressible axis in the tetragonal phase, shows a remarkable increase, or rebound, at P_c, almost as if a compressed structural spring had been released. The cell parameters then follow a curved path of decreasing slope, with continued compression, which must reflect a high compressibility and pressure derivative for cristobalite II.

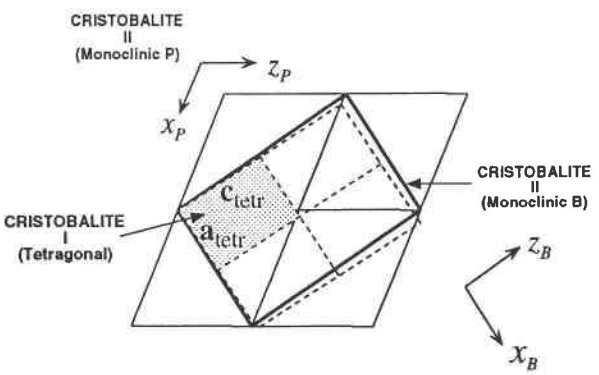

Fig. 2. Comparison of the low- and high-P phases of cristobalite (designated cristobalite I and II, respectively), projected onto (010). The low-P cell (shaded and with a dashed outline) is based on the extrapolation of tetragonal parameters to 3.1 GPa. Two settings of the monoclinic cell are shown.

Spontaneous strain

For a displacive phase transition involving a supergroup to subgroup relation, the order parameter, Q, may couple to the lattice strain. The resulting excess lattice distortion is characteristic of the phase transition and is usually expressed as the spontaneous strain, ϵ (Carpenter, 1992). Because one can never measure Q directly, measurements of macroscopic properties, such as the spontaneous strain, are essential for the thermodynamic description of phase transition behavior. The zone-boundary nature of the cristobalite I → II phase transition (accepting the change in space group from $P4_12_12$ to $P2_1$) leads us to expect quadratic coupling, $\epsilon \propto Q^2$ (in lowest order), to the spontaneous strain.

The symmetry of the spontaneous strain tensor is determined by point-group relations. The subgroups of 422 and the nonzero components of their spontaneous strain tensors are listed in Table 2. For the phase transition 422 → 2, the active representation is of type E (Janovec et al., 1975; Salje, 1990), comprising an orthogonal pair of basis functions. The xz (e_5) basis function describes a shear parallel to **a**, such that the angle β departs from 90° (Fig. 4a). The tetragonal condition $a = b$ is relaxed in the monoclinic system, and so an additional improper strain is allowed, involving extensions or contractions parallel to these two axes (i.e., nonzero e_{11}, e_{22}). This strain is subject to the constraint that there shall be no net volume change, and therefore we have the condition that $e_{11} = -e_{22}$.

The alternative basis function $yz - xz$ ($e_5 = -e_4$) is a shear parallel to [110] in the $(1\bar{1}0)$ plane of the tetragonal cell, leaving a unique (diad) axis perpendicular to the $(1\bar{1}0)$ shear plane (Fig. 4b). There is no longer any constraint that $\gamma = 90°$, and so an additional improper strain, e_{12}, is allowed. The resulting unit cell has $\alpha = \beta \neq 90°$ (because of e_{23} and e_{13}, respectively) and $\gamma \neq 90°$. This is better described by a conventional, monoclinic unit cell, with **b** perpendicular to the $(1\bar{1}0)$ shear plane of the tetragonal phase and with **a** and **c** lying within this plane.

The two distortion schemes and the unit-cell relationships are summarized in Figure 4. By comparing this figure with the actual monoclinic unit cell (and its pseudo-tetragonal relation) displayed in Figure 2, it is clear that deformation can be described by the xz basis function but not by the $yz - xz$ basis function.

We have described the spontaneous strain that violates

TABLE 2. Spontaneous strain relations for the subgroups of 422

Active repn.	Sub-group	Spontaneous strain: Proper	Spontaneous strain: Improper	No. elastic domains	Basis functions
A_2	4			1	z
B_1	222	$e_1 = -e_2$		2	$(x^2 - y^2)$
B_2	222	e_6		2	xy
E	2	e_5	$e_1 = -e_2$	4	x, y, xz, yz
E	2	$e_5 = -e_4$	e_6	4	
E	1	e_4, e_5	$e_6, e_1 = -e_2$	8	

Note: the monoclinic subgroups correspond to an orientation with the unique axis parallel to [010]; after Salje (1990).

the symmetry of the supergroup 422. In addition to this symmetry-breaking strain (e^{sb}), extra, non-symmetry-breaking strains (e^{nsb}) are allowed, which couple to the A representation of 422. These strains do not affect the off-diagonal (shear) terms of the strain tensor but may modify the on-diagonal terms, and hence, the unit-cell volume. From Table 2, we expect symmetry-breaking strains parallel to **a** and **b**, but not **c**; we may therefore express the axial strains as

$$e_{11} = e_{11}^{nsb} + e_{11}^{sb} \quad (3)$$

$$e_{22} = e_{22}^{nsb} + e_{22}^{sb} \quad (4)$$

$$e_{33} = e_{33}^{nsb}. \quad (5)$$

The non-symmetry-breaking strains must conform to the high-symmetry point group 422, and therefore we have the condition that

$$e_{11}^{nsb} = e_{22}^{nsb} \neq e_{33}^{nsb}. \quad (6)$$

Also, we already have a relation between two symmetry-breaking strain components (i.e., for no volume change) that

$$e_{11}^{sb} = -e_{22}^{sb}. \quad (7)$$

From these conditions, we arrive at the relations

$$e_{11}^{nsb} = \tfrac{1}{2}(e_{11} + e_{22}) \quad (8)$$

$$e_{11}^{sb} = \tfrac{1}{2}(e_{11} - e_{22}). \quad (9)$$

The phase transition involves a shear plus a volume

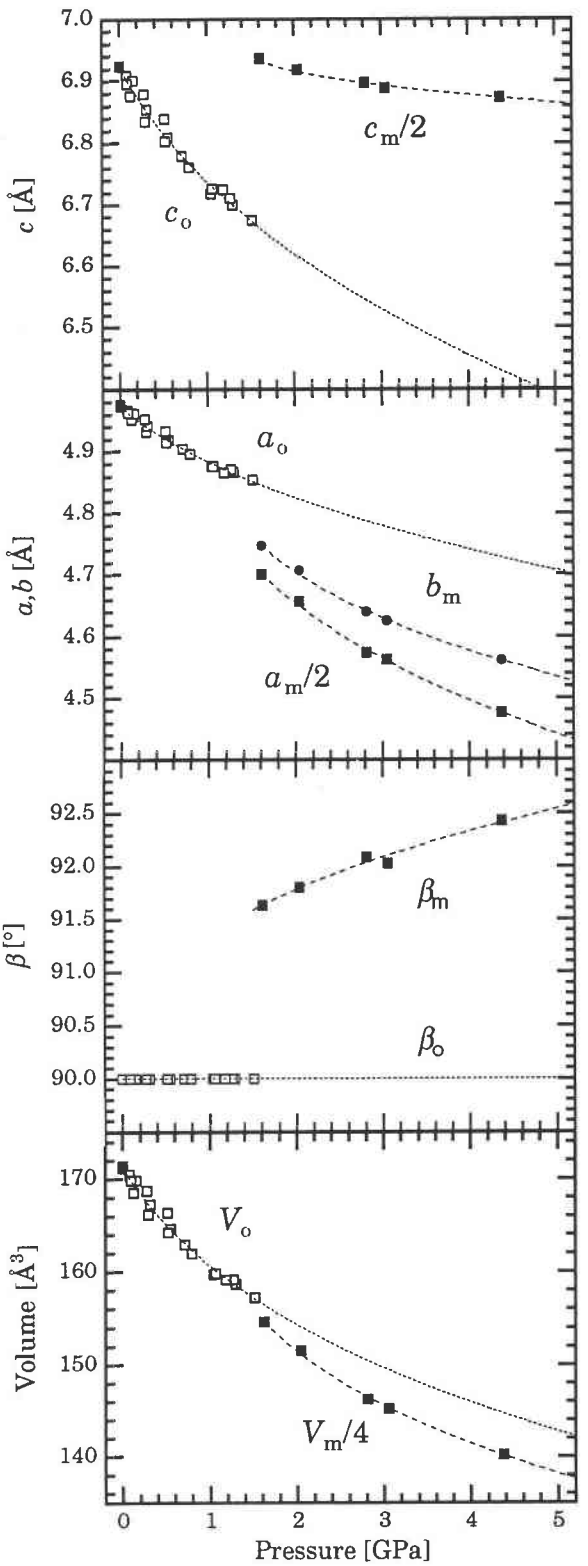

Fig. 3 Pressure dependence of the unit-cell parameters for cristobalite. The subscript 0 refers to the tetragonal phase and m refers to the pseudotetragonal setting of the monoclinic, cristobalite II phase. The solid symbols denote measurements from this study, using X-ray powder diffraction; the open symbols denote single-crystal X-ray diffraction measurements on the same sample, from Downs and Palmer (1994) (symbol size exceeds the experimental estimated standard deviations). The dashed lines through the tetragonal cell parameters a_0, c_0, and V_0 represent the best-fit Birch-Murnaghan-type functions and are used to extrapolate the tetragonal base lines into the stability region of the monoclinic phase.

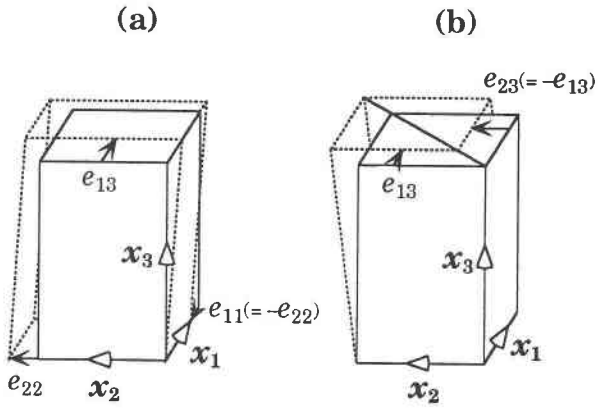

Fig. 4. Possible strain relations for the two distortion mechanisms characteristic of a phase transition from tetragonal 422 to monoclinic 2. The axial vectors of the undistorted tetragonal cell are indicated by $\mathbf{x}_1$–$\mathbf{x}_3$. (**a**) The *xz* basis function. The proper strain is e_{13}. Additional, improper strains, e_{22} and e_{11} ($= -e_{22}$) are allowed. (**b**) The *yz*-*xz* basis function. The proper strain is e_{13} ($= -e_{23}$). Additional improper strain, e_{12}, is possible (not illustrated here), which acts as a symmetrical shear of the unit cell, extending or compressing it parallel to [110], while preserving the diad perpendicular to the $(1\bar{1}0)$ plane.

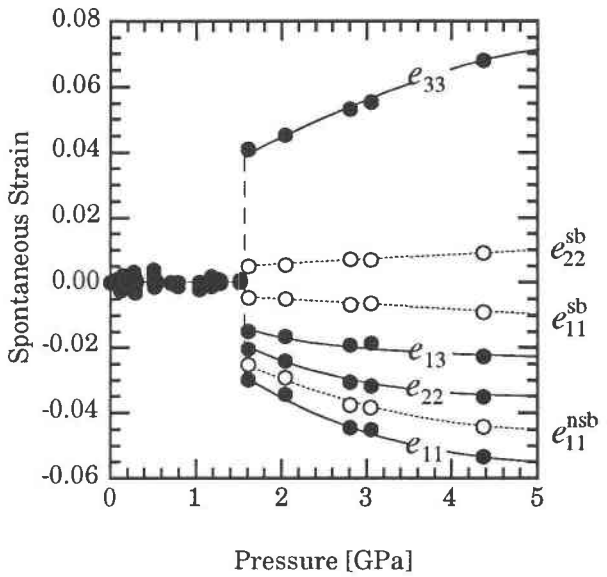

Fig. 5. Spontaneous strain components for monoclinic cristobalite. The solid symbols represent the measured lattice strains. The lattice strains parallel to **x** and **y** (e_{11} and e_{22}) involve symmetry-breaking $e_{11}^{sb} = -e_{22}^{sb}$ and non-symmetry-breaking components $e_{11}^{nsb} = e_{22}^{nsb}$, which are plotted as open symbols. The magnitudes of the e_{ij} calculated for data points below the phase-transition pressure give an indication of the uncertainties involved. The curves are guides for the eye to distinguish the different strain trends.

change. The measured strain tensor, **S**, can therefore be separated into symmetry-breaking and non-symmetry-breaking tensors:

$$\mathbf{S} = \begin{pmatrix} e_{11} & 0 & e_{13} \\ \cdot & e_{22} & 0 \\ \cdot & \cdot & e_{33} \end{pmatrix} = \begin{pmatrix} e_{11}^{nsb} & 0 & 0 \\ \cdot & e_{11}^{nsb} & 0 \\ \cdot & \cdot & e_{33} \end{pmatrix} + \begin{pmatrix} e_{11}^{sb} & 0 & e_{13} \\ \cdot & -e_{11}^{sb} & 0 \\ \cdot & \cdot & 0 \end{pmatrix}. \quad (10)$$

The symmetry-breaking strain tensor may be diagonalized to reveal the orientation (i.e., the shear plane) and magnitude of the corresponding strain ellipsoid.

The individual components of the spontaneous strain tensor may be calculated from the unit-cell parameters of cristobalite II, and those of cristobalite I extrapolated to the same pressure, using the general equations of Schlenker et al. (1978), summarized in Carpenter (1988). The spontaneous strain components are plotted in Figure 5. Note the very large non-symmetry-breaking strains e_{11}^{nsb}, e_{22}^{nsb}, and e_{33} in contrast to the rather smaller symmetry-breaking strains e_{11}^{sb} and e_{22}^{sb} and the shear strain, e_{13}.

Discussion

One of the crucial questions facing anyone trying to extend the Landau description of phase transitions to conditions of high pressure is the behavior of the excess volume. It transforms according to the identity representation A_1, which is proportional to Q^2 in lowest order, but there may be higher order dependencies on Q. For high-temperature phase transitions where the volume changes tend to be relatively small, the volume strain is observed, apparently without exception (Carpenter, 1992), to be proportional to the square of the order parameter. By contrast, at high pressures the volume changes are significantly larger, and one might expect to observe deviations from the ideal case $V_{ex} \propto Q^2$.

One can test for nonideality by directly comparing the pressure dependence of symmetry-breaking and non-symmetry-breaking (volume) strains. Because of the zone-boundary nature of the phase transition cristobalite I → II, both the symmetry-breaking strain (E representation) and the non-symmetry-breaking strain (A_1 representation, volume) are proportional to Q^2 in lowest order. In the absence of higher order terms, we would therefore expect linear scaling between the different strain components. However, if higher order coupling to the order parameter is significant, there is no longer any reason to believe that the various strain components will continue to scale linearly. (It is highly unlikely that individual strain components would have identical coupling constants). Figure 6 demonstrates that $e_{13} \propto e_{33}$, indicating that either these components have identical higher order couplings to the order parameter (which would be exceedingly fortuitous), or, as seems more likely, there are no significant higher order coupling terms at all—in which case, the volume-changing strain remains proportional to the square of the order parameter. That is despite the fact that cristobalite is an example of a system with much

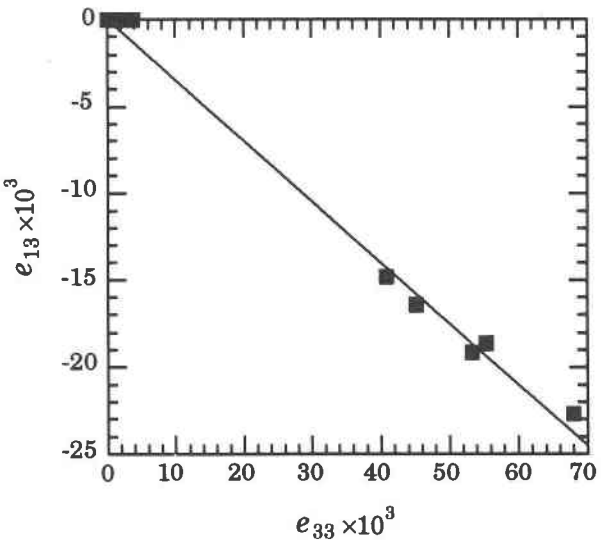

Fig. 6. Symmetry-breaking strain component (e_{13}) as a function of a non-symmetry-breaking strain component (e_{33}). The two strains scale linearly with each other, reflecting their dependence on the square of the macroscopic order parameter for the tetragonal to monoclinic phase transition.

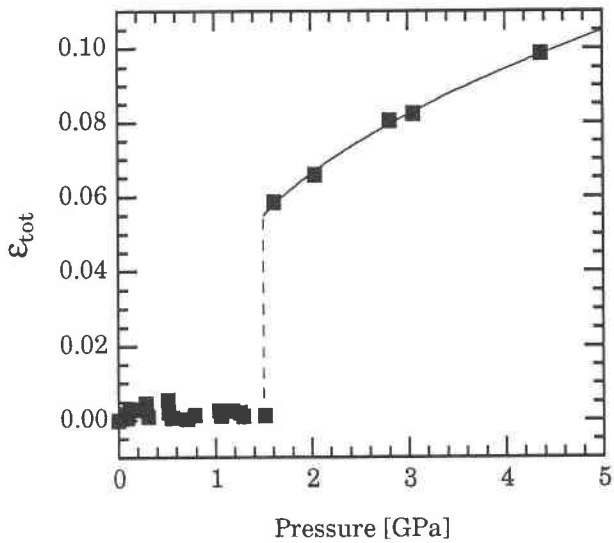

Fig. 7. Pressure dependence of the total spontaneous strain, ϵ_{tot}. The solid line represents the best-fit Landau function corresponding to $\epsilon \propto Q^2$ for a first-order phase transition. The magnitude of ϵ_{tot} calculated for data points below the phase transition pressure gives an indication of the uncertainties involved.

larger spontaneous strains (~6–10% for ϵ^{nsb} and 2–4% for ϵ^{sb}) than is typical for proper ferroelastics (~2%) and improper ferroelastics (<1%).

Because the strain components are observed to be all proportional to each other, the overall spontaneous strain ellipsoid must change in size, but not orientation, with changing P and T. For the total strain (including symmetry-breaking and non-symmetry-breaking components), the principal axis of the tensor is found to remain at about $\theta_x^{tot} = 10°$ to the x axis, while the ellipsoid of the symmetry-breaking strain remains oriented at approximately $\theta_x^{sb} = 40°$ to the x axis for all pressures. For ferroelastic phase transitions we consider the strain-order parameter coupling only, leading to renormalized elastic constants, reflecting the inverse susceptibility. Because the orientation of our strain ellipsoids is invariant with pressure, we can confidently state that the strain-order parameter coupling is invariant over this pressure range. This high-pressure phase transition can therefore be treated in the same Landau manner as many high-temperature structural phase transitions.

Because of the constant ϵ-Q coupling, it is valid to calculate a total, scalar spontaneous strain from the different strain components. There are various definitions for such a strain, but perhaps the most commonly used one (e.g., Redfern and Salje, 1987; Carpenter, 1988; Salje, 1990) is

$$\epsilon_{tot} = \sqrt{\sum_{i=1}^{6} e_i^2} \qquad (11)$$

where e_i are the components of the spontaneous strain tensor derived above. The total strain, proportional to Q^2, is plotted in Figure 7 and shows good agreement with this first-order Landau model. The size of the step in ϵ at the phase transition is particularly important: it is proportional to the ratio of the Q^2 and Q^4 coefficients in the Landau potential. By combining this information with further measurements of other macroscopic properties, it will be possible to construct the effective Landau potential, and hence obtain the thermodynamic implications of the phase transition cristobalite I → II.

The orientation of the symmetry-breaking strain ellipsoid is intriguing. The extensional axis (ϵ_1) is parallel to $[\bar{1}01]$ in the (101) plane of the tetragonal phase: a plane of distorted six-membered tetrahedral rings, which in the high-temperature cubic phase, becomes the pseudo-close-packed (111) plane. This direction is equivalent to $[\bar{1}\bar{1}2]$, precisely the slip direction one would expect for the smallest possible shear of the {111} layers. The cristobalite I → cristobalite II phase transition can therefore be viewed as a shear of the crystal structure, involving the sliding of adjacent close-packed sheets against each other, much as in the martensitic-type transformations of close-packed metals. Such transitions give rise to a defect microstructure, and one might predict the formation of stacking faults, and even glide twinning. In our single-crystal diffraction work on the high-pressure phase of cristobalite (Palmer and Downs, 1991), we observed split single-crystal diffraction peaks, as measured in ω and $\theta/2\theta$ scans, indicative of such twinning. In addition, repeated cycling of the crystal through the phase transition, followed by quenching to ambient pressure, yielded a twinned, tetragonal crystal, whereas the original tetragonal crystal, before pressure treatment, had been untwinned. These deformation twins must be distinct from the tetragonal to monoclinic transformation twins, as the

latter cannot exist in the tetragonal phase. Further evidence for a strain-related, deformation microstructure is the coexistence of both high- and low-pressure phases within the hysteresis region, observed in the single-crystal X-ray experiments (Downs and Palmer, 1994) and Raman spectroscopy experiments (Palmer et al., 1991). The underlying microstructure should be revealed by transmission electron microscopy, and a systematic study of cristobalite before and after phase transition cycling would be very rewarding.

Acknowledgments

We would like to thank the Harvard Mineralogical Museum for its loan of the sample. David Cox and Andrew Jephcoat provided invaluable assistance during the synchrotron X-ray experiments. Michael Carpenter, Ekhard Salje, and Charles Prewitt are to be thanked for their helpful comments. The manuscript was greatly improved by reviews from Ross Angel, Andrew Christy, and an anonymous reviewer. The National Synchrotron Light Source (Brookhaven National Laboratory) is supported by the U.S. Department of Energy, Division of Materials Sciences and Division of Chemical Sciences (DOE grant DE-AC2-76CH00016). This research was funded by the National Science Foundation (NSF grants EAR-22-34530 to L.W.F., and EAR-91-17433 to C.T. Prewitt and D.C.P.) and by the Carnegie Institution of Washington.

References cited

Carpenter, M.A. (1988) Thermochemistry of aluminium/silicon ordering in feldspar minerals. In E.K.H. Salje, Ed., Physical properties and thermodynamic behaviour of minerals, p. 265–323. Reidel, Dordrecht, The Netherlands.

——— (1992) Thermodynamics of phase transitions in minerals: A macroscopic approach. In G.D. Price and N.I. Ross, Eds., The stability of minerals, p. 172–216. Chapman and Hall, Boston, Massachusetts.

Dollase, W.A. (1965) Reinvestigation of the structure of low cristobalite. Zeitschrift für Kristallographie, 121, 369–377.

Dove, M.T., Giddy, A.P., and Heine, V. (1992) On the application of mean-field and Landau theory to displacive phase transitions. Ferroelectrics, 136, 33–49.

Downs, R.T., and Palmer, D.C. (1994) The pressure behavior of α cristobalite. American Mineralogist, 79, 9–14.

Giddy, A.P., Dove, M.T., Pawley, G.S., and Heine, V. (1993) The determination of rigid unit modes as potential soft modes for displacive phase transitions in framework crystal structures. Acta Crystallographica, A49, 697–703.

Hatch, D.M., and Ghose, S. (1991) The α-β phase transition in cristobalite, SiO_2. Symmetry analysis, domain structure, and the dynamical nature of the β-phase. Physics and Chemistry of Minerals, 17, 554–562.

Janovec, V., Dvorak, V., and Petzelt, J. (1975) Symmetry classification and properties of equi-translation structural phase transitions. Czech Journal of Physics, B25, 1362–1396.

Jephcoat, A.P., Finger, L.W., and Cox, D.E. (1992) High pressure, high resolution synchrotron diffraction with a position-sensitive detector. High Pressure Research, 8, 667–676.

Mao, H.K., Bell, P.M., Shaner, J. W., and Steinberg, D.J. (1978) Specific volume measurements of Cu, Mo, Pd, and Ag and calibration of the ruby R_1 fluorescence pressure gauge from 0.06 to 1 Mbar. Journal of Applied Physics, 49, 3276–3283.

Palmer, D.C., and Downs, R.T. (1991) High pressure behavior of cristobalite revealed by single-crystal x-ray diffraction (abs.). Eos, 72, 478.

Palmer, D.C., Downs, R.T., and Hemley, R.J. (1991) High pressure phase transitions in cristobalite: Condensed Matter and Materials Physics (CMMP91), 17–19 December 1991, Birmingham, England. The Institute of Physics Abstracts with Program, 53.

Peacor, D.R. (1973) High-temperature single-crystal study of the cristobalite inversion. Zeitschrift für Kristallographie, 138, 274–298.

Redfern, S.A.T., and Salje, E.K.H. (1987) Thermodynamics of plagioclase. II. Temperature evolution of the spontaneous strain at the $I\bar{1}$-$P\bar{1}$ phase transition in anorthite. Physics and Chemistry of Minerals, 14, 189–195.

Salje, E.K.H. (1990) Phase transitions in ferroelastic and co-elastic crystals, 366 p. Cambridge University Press, Cambridge, England.

Schlenker, J.L., Gibbs, G.V., and Boisen, M.B. (1978) Strain-tensor components expressed in terms of lattice parameters. Acta Crystallographica, A34, 52–54.

Schmahl, W.W., Swainson, I.P., Dove, M.T., and Graeme-Barber, A. (1992) Landau free energy and order parameter behaviour of the α/β phase transition in cristobalite. Zeitschrift für Kristallographie, 201, 125–145.

Stokes, H.T., and Hatch, D.M. (1988) Isotropy subgroups of the 230 crystallographic space groups, 580 p. World Scientific, Singapore.

Swainson, I.P. (1992) The phase transition and dynamic disorder in cristobalite. Ph.D. thesis, University of Cambridge, Cambridge, England.

Tolédano, J.-C., and Tolédano, P. (1987) The Landau theory of phase transitions, 451 p. World Scientific, Singapore.

Tsuchida, Y., and Yagi, T. (1990) New pressure-induced transformations of silica at room temperature. Nature, 347, 267–269.

Van Valkenburg, A., and Buie, B.F. (1945) Octahedral cristobalite with quartz paramorphs from Ellora Caves, Hyderabad State, India. American Mineralogist, 30, 526–535.

Werner, P.-E., Eriksson, L., and Westdahl, M. (1985) TREOR, a semi-exhaustive trial-and-error powder indexing program for all symmetries. Journal of Applied Crystallography, 18, 367–370.

Wolfe, C.W. (1945) Crystallography of cristobalite from Ellora Caves, India. American Mineralogist, 30, 536–537.

Wright, A.F., and Leadbetter, A.J. (1975) The structures of the β-cristobalite phases of SiO_2 and $AlPO_4$. Philosophical Magazine, 31, 1391–1401.

Yeganeh-Haeri, A., Weidner, D.J., Parise, J., Ko, J., Vaughn, M.T., Liu, X., Zhao, Y., Wang, R., and Pacalo, R. (1990) A new polymorph of SiO_2 (abs.). Eos, 71, 1671.

Yeganeh-Haeri, A., Weidner, D.J., and Parise, J.B. (1992) Elasticity of α-cristobalite: A silicon dioxide with a negative Poisson's ratio. Science, 257, 650–652.

Manuscript received April 13, 1993
Manuscript accepted August 26, 1993